STRUCTURAL ANALYSIS OF A CENTRE BOX OF A VERTICAL TAIL PLANE WITH A SIDE PANEL FROM COMPOSITE FOAM SANDWICH

M. I. Zuardy, FIBRE, Airbus-Strasse 1, 21684 Stade, Germany
T. B. Block, FIBRE, Am Biologischen Garten 2, Gebäude IW3, 28359 Bremen, Germany
A. S. Herrmann, FIBRE, Am Biologischen Garten 2, 28359 Bremen, Germany

Abstract

Sandwich panels are increasingly used in aircraft structures due to their high specific bending stiffness and hence excellent buckling stability. The objective of this work is to find rough sizing process of a composite sandwich panel incorporating multi-scale modelling techniques to substantiate structural capability of each level of test pyramid, and find a minimum number of tests required to validate the approaches. The numerical analysis of such hybrid structures by means of the finite element method (FEM) requires specific strategies regarding the degree of homogeneity of each component. The common modelling approach for solid laminate of carbon fibre reinforced plastics (CFRP) structures using an extended layered shell element formulation can also be applied in modelling of sandwich panels in the global FE-model. The sandwich core, which is thicker compared to the solid laminate CFRP skins, can be formulated as an additional layer between the two face skin layers. For more detailed modelling of the sandwich structure, e.g. a cut out of the global FE model (GFEM), a solid shell approach can be applied. Both of the monolithic skins are idealised using layered shell, while the sandwich core is represented by solid elements. For a hard foam core the solid elements are assigned to the core system according to their type, isotropic material for unreinforced foam or homogenised, anisotropic properties for a reinforced foam core system. The homogenised mechanical properties of the reinforced foam core can be determined using analytical or numerical approaches, in which for a numerical approach the textile profile or needles shaped foam reinforcements are modelled with shell and beam elements respectively. With some modifications the meso-mechanical FE-model can further be used e.g. through the application of explicit FEM for the determination of an impact damage or using the virtual crack closure technique (VCCT) method and a higher level of FE discretisation to assess the growth behaviour of damages. The non-linear FE analyses show a good agreement with the recorded panel deformations.

Keywords: Composite sandwich, foam core reinforcement, VTP centre box, damage tolerance, test pyramid, multi-scale modelling, nonlinear FE-Analysis, buckling stability, impact simulation, debonding growth

1. INTRODUCTION

When we consider a stiffened monolithic shell structure, we can regard a sandwich panel in the sense of optimized lightweight design as smearing of the longitudinal and transverse stiffeners, in which the one stiffener flanges are smeared in the shell structure and the other stiffener flanges are merged together into an additional shell structure and the stiffener webs are merged into a continuous core or spacer material between the first shell and the newly formed shell [1]. Because of the second shell constructed in this way, the sandwich structure is also called "double shell structure" in the literature [2].

Various types of core structure are inserted between the two shells, such as hard foam, honeycomb, tube core, corrugated sheet or folded core and "nab honeycomb", etc. The comparable continuous reinforcing effect of the core in all directions gives the sandwich panel better local stability characteristic than those provided by a discretely reinforced or stiffened monolithic shell. In the latter case, the shell zone between the stiffeners, also known as stiffener bay, tends to suffer a local problem with buckling when the structure is subjected to compression or shear loading or a combination thereof. A transition structure between sandwich and stiffened monolithic is the so-called isogrid panel. In FIG. 1 structural masses of various shell constructions as a function of allowable axial compression are compared. A lower structural weight than the sandwich can be realised with a corrugated shell structure, which is however not significant for an application in aviation technology due to aerodynamic reasons [3].

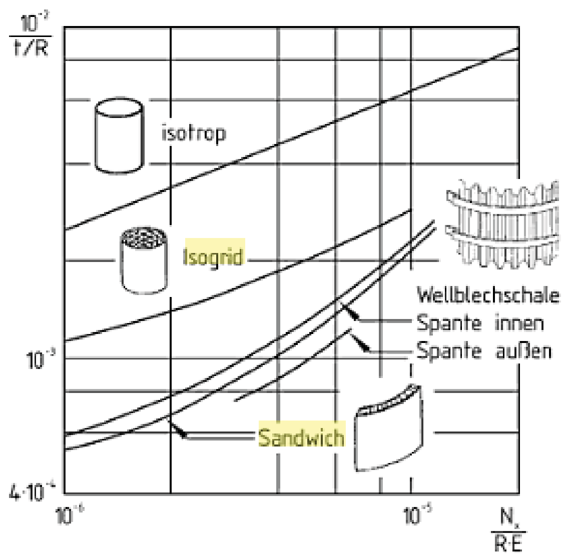

FIG. 1. Weight comparison between various shell constructions under axial compression load [3]

1.1. Aspects of Structural Stability

Depending on the core type in place, the sandwich structure experiences local instability or failure modes initiated by certain boundary conditions. Among these are buckling of the cell walls in the case of corrugated or honeycomb cores, and short-wave wrinkling of the skins if the honeycomb cell size exceeds a critical value [4]. The local instability modes can be analytically calculated using formulas from standard structural handbooks, such as HSB[1], ESDU[2] or MIL-HDBK. These instability modes could excite the growth of damage, but fortunately have not been observed within the sandwich configuration in this work. Therefore, only the global stability modes of a sandwich panel are considered, which may affect the bonding elements and lead to overall structural failure. For a simplified geometry the analytical method delivers relatively quick and accurate results, which can be plotted for combined axial shear-compression with and without transversal shear loads into a so called interaction curve (FIG. 2).

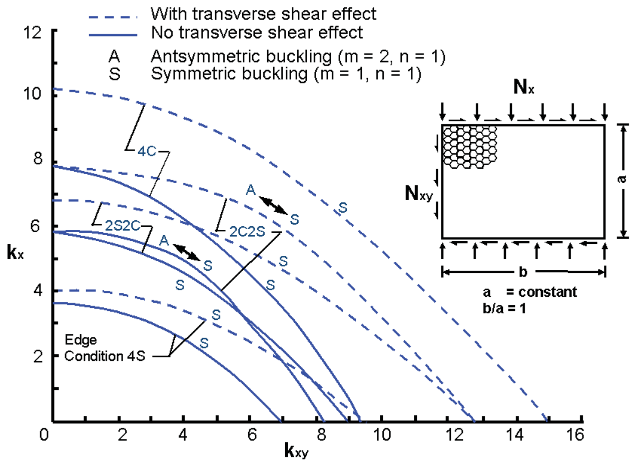

FIG. 2. Interaction curves of a honeycomb sandwich [5]

1.2. Aspects of Damage Tolerance (DT)

As shown in the FIG. 3 the knowledge of the dependency of residual strength to certain damage sizes[3] based on the detectability is the basis of DT, which is an important issue for the certification of composite primary structures. Apart from the inspection method, this procedure applies also for a composite foam core sandwich structure.

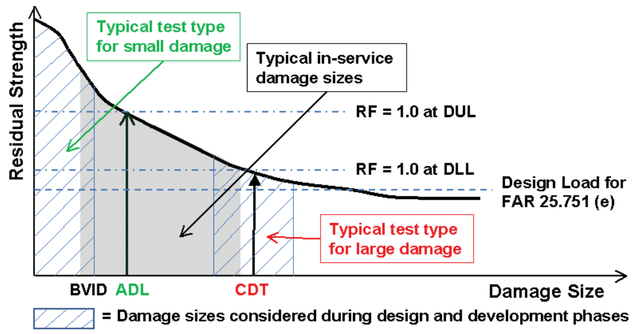

FIG. 3. Residual strength versus damage size [6]

Due to the heterogeneous nature of a sandwich structure, this type of core composite is very sensitive to a concentrated local stress, such as impact loading[4]. More damage modes are possible than in case of a monolithic structure. The top face skin will be usually *delaminated* like monolithic composite and also *debonded* due to the *crushed core* and *cracked interface* resin respectively (FIG. 4). **Note:** The bottom skin remains normally undamaged.

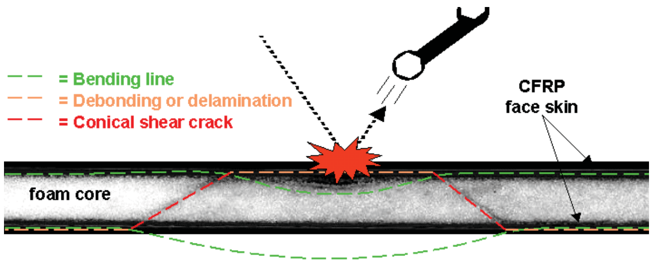

FIG. 4. Possible damage modes of composite foam sandwich due to impact loading

When a conical shear fracture occurs due to a high shear angle initiated through localised bending deformation, the enclosed core zone is completely separated from the remaining core system. Furthermore, the conical shear fracture may provoke a *secondary debonding* in the interface zone where the top skin faces away from the direction of the impact; therefore this is the critical type of impact damages. A preliminary investigation to predict the possible impact damage modes was carried out in [7].

A damaged core zone under the face skin is difficult or completely impossible to detect it visually due to its concealed location. Therefore, in this research work the impact behaviours are numerically investigated by means of explicit FE analyses first on small sandwich specimens and later transferred to large-scale components. In parallel, non-visual inspection methods are developed, i.e. air coupled ultra sonic transmission scanning or pulse-echo.

The knowledge on the effects of these damages is considered a challenge [8]; it is investigated in this research work together with the stability behaviour in order to proof the structural integrity. Otherwise, an isogrid panel as shown in FIG. 1 would be more advantageous.

2. DESIGN AND ANALYSIS CONCEPT OF THE CENTER BOX OF A VERTICAL TAIL PLANE

The design depicted in the patent sketch, FIG. 5, is used as a baseline design for the development of the centre box in the aircraft research program[5] initiated by the Federal Ministry for Industry and Technology of Germany (BMWi), under the project "LoKoST". The distinctive feature of the so-called coupled frame rib in the novel design concept is that it simplifies the manufacture and assembly of the centre box because of the lower tolerance compensation required. Furthermore the frame rib together with the rudder hinges, forms a complete framework system guaranteeing the required form or torsional stability of the centre box. The shear wedge connecting both of the half frame ribs closes the shear load path and should sustain the brazier load due to global bending of the centre box.

[1] Handbuch Struktur-Berechnung
[2] Engineering Sciences Data Units
[3] Allowable Damage Limit: ADL; Critical Damage Threshold: CDT

[4] Also known as accidental damage
[5] Luftfahrtforschungsprogramm abbreviated as LuFo

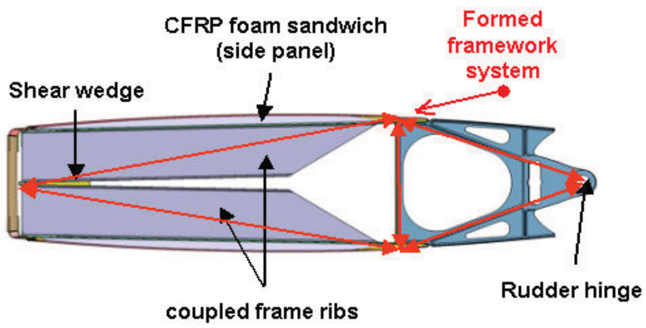

FIG. 5. Centre box with coupled frame rib and the formed framework system (red line) [9]

2.1. CFRP Foam Core Sandwich Configuration

The specific part of the mentioned centre box is its side panel, which is conceived as sandwich design. Hence, it would be the first large-scale primary sandwich structure and is the main focus of this research work. The side panel has a curved outer skin (loft) and flat inner skin; this produces the so-called "lenticular" cross-section. The so constructed composite sandwich side panel has for various reasons an excellent impact damage resistance and good structural behaviour [10]. In order to enhance the damage tolerance, the foam core is provided with CFRP reinforcements. There are three different types of reinforcement shown in FIG. 6 that can be considered.

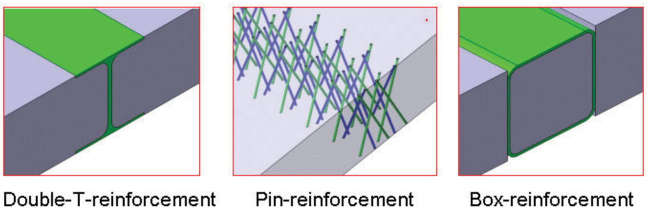

FIG. 6. Reinforcement concepts for foam core

Primarily the compression strength after an impact load (CAI-strength[6]) shows an improvement when compared to the unreinforced sandwich configuration. Other pin configurations can be found in [11], where Kevlar fibres are stitched in the foam core using the lock stitch method.

2.2. Structure Development Approach

As it is standard practice in structural development in aviation technology, a number of structural and mechanical tests required for the development and certification of the final configuration of the advanced VTP centre box.

2.2.1. The Test Pyramid

In composite structures, since "the material is not pre-existent to the part itself", a multilevel approach[7] is necessary [12]. This type of approach, first used for metal aeronautic structures, is set out in a "test pyramid" in Europe [13]. The width of each pyramid level shows the proportionality-required number of specimens, but reciprocally to the cost and complexity as shown in FIG. 7. While it takes hundreds of samples for the characterisation of sandwich technology and determination of the basic structural properties in generic tests in the coupon and element level (E & D), it remains only a dozen of test components with the technology specific detailed experiments (C). On the very specific level of sub-components (B), only some components have to be tested and on the top-level component (A) for the detection of static, fatigue and DT respectively only a single test is required. The expensive real tests are being increasingly substituted by virtual tests, in which the missing data are interpolated by means of FE analyses.

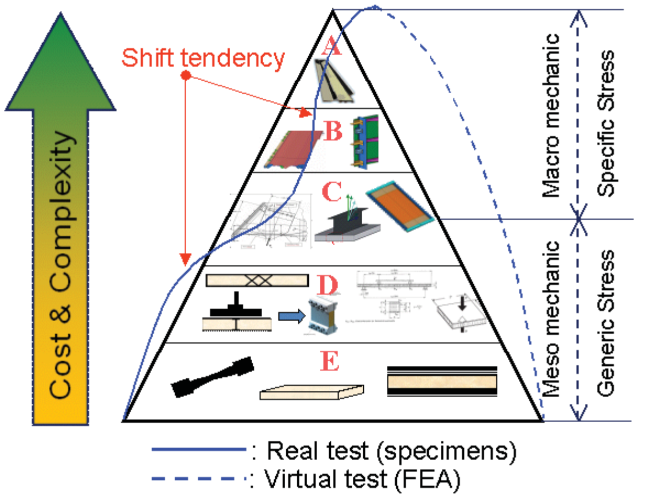

FIG. 7. Test pyramid, based on Rouchon [13] with the tendency of application of virtual testing [14].

2.2.2. The Numerical Calculation

For verification of the tests and the development of the structural calculation method, state of the art FE analyses are performed throughout the test pyramid. The FE method is briefly explained in the following section.

2.2.2.1. The Finite Element Method (FEM)

The Finite Element Method is a numerical method for solving various problems in structural mechanics, concerning both static and dynamic issues. Starting with energy principles, the component or problem area to be investigated is divided into a number of finite elements that are connected to each other with node or grid points at the element edges. The displacements and deformations within the element are approximated by constitutive equations from the displacements of the individual nodes, the so-called shape functions. The construction of shape functions is normally determined by the intended use. Because of the matrix-form of the system equations, it can be reasonably solved using numerical computation [18].

The equilibrium relationship in elastostatics can be expressed with the following well-known equation:

$$(1)\quad \int_V \delta \underline{u}^T \underline{\underline{D}}^T \underline{\sigma} dV + \int_V \delta \underline{u}^T \underline{X} dV = 0$$

And the constitutive equation as a function of nodal displacement ($\underline{u}$):

$$(2)\quad \delta \underline{u} = \sum \underline{\underline{N}}_i \delta \underline{u}_i = \underline{\underline{N}} \cdot \delta \underline{u}^e$$

The following general equation can be deduced:

$$(3)\quad \delta(\underline{u}_e)^T \int_V \underline{\underline{N}}^T \underline{\underline{D}}^T \underline{\underline{E}}\,\underline{\underline{D}}\,\underline{\underline{N}} dV \cdot \underline{u}^e - \delta(\underline{u}_e)^T \int_{O_p} \underline{\underline{N}}^T \underline{p} dO_p + \delta(\underline{u}_e)^T \int_V \underline{\underline{N}}^T \underline{X} dV = 0$$

[6] Compression (strength) After Impact
[7] Building block approach

The integral form can be converted into a matrix form:

$$(4)\quad \underline{\underline{K}}^{e}\,\underline{u}^{e} - \underline{P} = 0$$

In other words, a *stiffness matrix*, the displacements and the forces applied to each node, can describe the complete equation system. The equation is furthermore a typical *eigenvalue* problem. The solution according to the eigenvalue analysis (e.g.: by the *Lanczos* method), gives the eigenvalue (λ), which, after multiplication with $\underline{P}$ represents the critical buckling load N_X and the corresponding *eigenvector* ($\underline{u}$), i.e. the buckling mode.

For large structural deformations, a function of the stiffness matrix in dependency to $\underline{u}$, the so-called geometrical or differential stiffness should be considered:

$$(5)\quad \left(\underline{\underline{K}}_{L} + \underline{\underline{K}}(\underline{u})^{e}\right)\underline{u}^{e} - \underline{P} = 0$$

The solving of this equation is therefore known also as *geometrical non-linear* analysis. In the context of stability analysis, the solution is again performed on the basis of the eigenvector ($\underline{u}$) with additional minimal disturbance[8] and can be solved by incremental *iterative* formulas, such as the *Newton-Raphson* method (FIG. 8 LH). For a snap-through problem that normally arises when curved shells buckle, the better solution is the *Riks* method or its modification due to the abrupt change of the gradient of the solution curve near the bifurcation points (FIG. 8 RH).

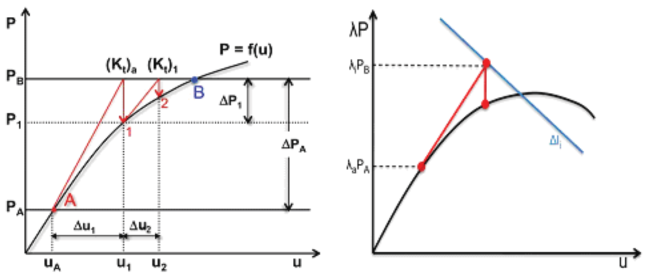

FIG. 8. Newton-Raphson and modified Riks solution method [19]

For time dependent problems, such as transient dynamic process, a *time-integration* is additionally required. In case of high frequency process and many contact surfaces, such as an impact event, the use of *explicit* time integration is more advantageous. For low rate process, such as damage growth, *implicit* schema is more suitable.

2.2.2.2. Meso-/Macro-Mechanic Approach

The modelling of a pin- as well as profile reinforced core system can be realised in different degrees of detail. So it is possible to describe the pin-reinforced foam core with discrete formulated pins inside the foam elements (*meso mechanic*). Here, the pins are formulated as volume or beam element. The latter are advantageous in simulation of large-scale sandwich structures due to computational effort by the complexity. Another possibility is a so-called two-scale simulation, in which a periodically repeating unit cell (RUC[9]) is simulated with high accuracy but also high cost. The results are then assigned to the material card of the core system of a large FE model (*macro mechanic*) [10]. The different approaches are summarized in TAB 1.

	Unit Cell (UC) 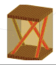	Discrete Pin Modeling 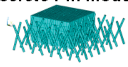	Homogenised Core System 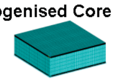
Model	Smallest UC possible	Coupon or element level	Detail- upto component level
Pro	Detailed understanding	Relatively deeper understanding	Low modeling and computational effort
Con	Very high modeling effort	Relatively High modeling effort	Requires analytical or FE approach to homogenization

TAB 1. Modelling approaches for reinforced foam core

In case of double-T-reinforcement, the elements of reinforcement can easily be incorporated into the existing FE model of the composite foam sandwich.

2.2.2.3. Global-/Local FE Modelling Approach

The development process of numerical calculation operates in the opposite way to the structural tests; from the global computation model (GFEM) to more detailed component models. The composed entire computation model, the so-called global FE-Model (GFEM) representing the global stiffness behaviour is broken down into some smaller and more detailed models, the so-called discrete FE-Models (DFEM). The global aerodynamic loads act only on the surface nodes of the GFEM. The sizing process is carried out locally in each of the DFEMs. With this global-local modeling strategy the required section loads for the components to be tested can be deduced.

2.2.2.4. Loads Definition of the GFEM

In the early phase of aircraft development, where no actual aerodynamic loads were available, the shear moment torsion (SMT) loads were applied for preliminary analysis. These loads are resulted from the calculation of simplified aircraft model using beam and concentrated mass elements as depicted in FIG. 9, i.e. GFEM for load extraction. The loads acting on the elastic axes or shear centres of the centre boxes are distributed via kinetic constraints or rigid-body elements (MPC[11]) through the rib attachments.

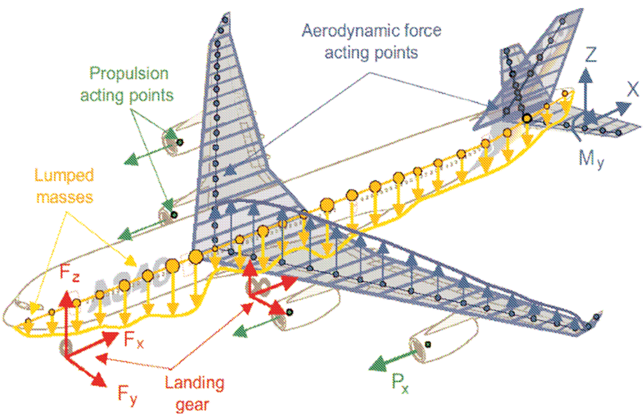

FIG. 9. A simplified FE-beam model (1D) with concentrated mass (0D) of the entire aircraft [15]

[8] Imperfection
[9] Representative Unit Cell
[10] Multi scale approach: micro-/meso-/macro mechanic al model
[11] Multi Point Constrains

In the design of the vertical tail plane under consideration, its outer contour (profile) and corresponding aerodynamic loads are based on a certified reference aircraft, on which the necessary flight scenarios and corresponding surface loads already exist. In the context of this research, in order to reduce the number of load cases to be considered as a function of flight status, it is necessary to extract so-called enveloping or significant load cases from the total number of load cases that can arise.

2.2.2.5. Construction of the GFEM

Considering a sensitivity study or optimisation, the GFEM is usually modelled using shell elements. This approach allows simple change of the GFEM. The foam core, which is thick in comparison with the face skin, can be defined as an additional laminate layer of the material card[12], where its thickness for each element is assessed directly from the CAD drawing data base by means of computer scripts and assigned accordingly. Because of the lenticular cross-section of the sandwich side panel, FE meshing results in a stepwise topography and there is a discontinuous or jump in rigidity between the neighbouring elements within the mesh of the side panel. Numerically this rigidity jump leads to apparent local buckling modes that are insignificant within the structural stability analysis.

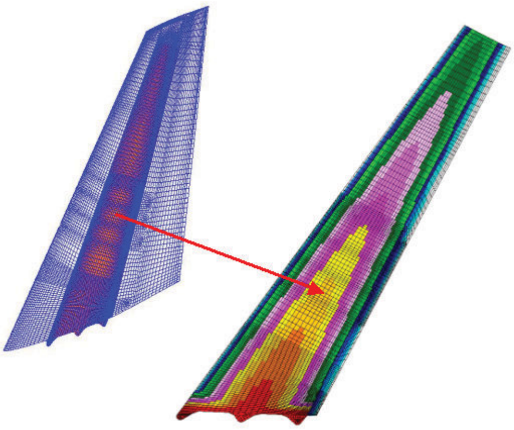

FIG. 10. The GFEM of the VTP centre box with the stepwise mesh topography (thickness plot)

The lenticular cross-section of the side panels allows for two shell modeling strategies:

1. Modelling of the shell elements on the curved outer skin of sandwich side panels, where a cavity arises between the shell and the frame rib. The section loads from the shell are then transferred to the half frame rib via MPC.

2. Modelling of the shell elements on the flat inner skin of sandwich side panels. The side panels and the flange of the frame rib lie on top of each other and no MPC is needed for load transfer. The disadvantage is the need to interpolate the aerodynamic loads on the outer curved sandwich skin (loft) to the inner flat side of the panel, which represents now the sandwich shell. Furthermore, the centre box is somewhat more bending flexible due to the smaller moment of inertia relative to the neutral plane.

[12] Material card (MAT) of NASTRAN

In order to investigate the global buckling stability of the centre box, the stiffness of the neighboring structures, such as leading and trailing edges are transferred via the corresponding nodes by means of so-called free body loads[13]. As anticipated, the stability analysis resulted in a higher buckling load (*eigenvalue*) in the first GFEM (λ = 2.05) than in the second (λ = 1.84). This relatively high buckling value of the baseline configuration provides enough design space for a global structural optimization.

2.2.2.6. Critical Sandwich Areas (DFEM)

The mentioned critical buckling zone of GFEM was modelled in detail. Using the sub-structure technique, section loads were transferred from the GFEM through free body loads (FIG. 11 LH).

a). Test Area for The Buckling Stability

The linear stability calculation as carried out in the DFEM gives a buckling value (λ) of **1.83** as shown in the FIG. 11.

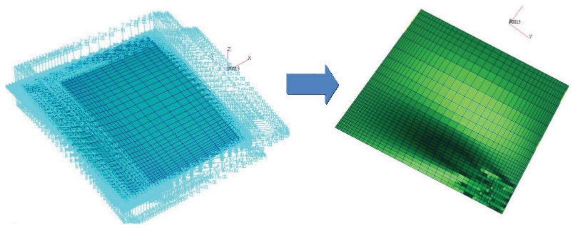

FIG. 11. Detailed buckling investigation of the critical zone by means of the sub-structure technique

An analytical comparison calculation is then carried out with the help of the buckling formula for orthotropic plates from HSB [16]. This transforms the trapezoid section into a virtually equivalent quadrilateral together with the averaged section loads. The effective plate rigidity values ($\mathbf{D}_{eff}$) are determined using classical laminate theory (CLT). The calculated buckling value or reserve factor (λ) = **1.825** shows close agreement with the numerical analysis and demonstrates that this simplified analytical formula can be used as a corollary in the general setting of global FE analysis, for a rapid assessment in a sensitivity study.

b.) Test Area for Load Introduction

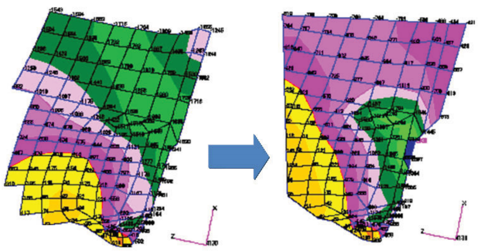

FIG. 12. Derivation of the test panel of main lugs with the corresponding nodal loads (not scaled)

Furthermore, because of the complexity of its structure configuration, the cutout of transitional or load introduction area for transferring concentrated loads into the composite sandwich shell were examined together with sectional loads from the GFEM.

[13] Loads of free body diagram (sub structuring)

2.2.3. Test Specimens and Their Arrangements

The stability-critical zone of the side panel, as mentioned, is too large to fit the existing test installation (FIG. 13). Also, because of the lenticular shape of the cross-section as a result of the symmetry requirements, no further sub-divisions can be generated. The test panel is therefore derived from the other sandwich detail and modified to produce a symmetrical test component.

The resulting sandwich panel consists of a flat inner skin and a curved outer skin of CFRP. The adoptions of the closed-cell hard foam as the sandwich core and non-crimp fabrics (NCF) as the face skin facilitate manufacturing using a standardised resin infusion process (MVI[14]). Metal brackets bolted to the monolithic longitudinal edges (MLEs) of the panels were used to introduce shear loads in the longitudinal direction ($\mathbf{F}_{SV}$). Further metal brackets on the front face (plugged with thick resin) were used to introduce axial compression loads ($\mathbf{F}_C$) and shear loads in the transverse direction ($\mathbf{F}_{SH}$). Two aluminium stiffeners (dummy ribs) were bonded onto the flat inner skin. The area between the two dummy ribs and MLEs represents the test zone. Arms bonded to the stiffeners supported the positioning of the panel in the through-thickness direction. A special mobile impact device was used to apply impact loads to the panel held firmly in the test installation.

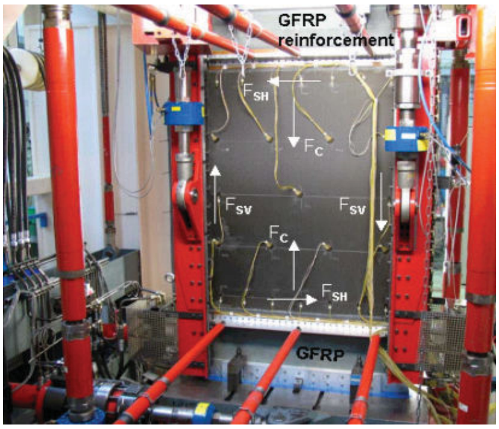

FIG. 13. Arrangement of shear-compression test with support arms and load introductions [17]

The test arrangements and test parts for VTP load introductions are similar to the mentioned shear-compression test. The test facilities are relatively simple in this case, since no in-plane shear loading is to be introduced.

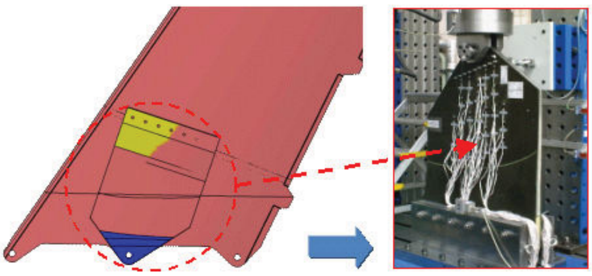

FIG. 14. Derivation of test component for main lug (LH) and its test arrangement (RH)

For the load introduction to the rudder, the dummy bracket should be able to withstand high actuator load during simulated system failure (jamming or force fighting).

3. INVESTIGATION OF COUPON AND ELEMENT SPECIMENS (MESO-MECHANIC)

The investigations on coupon and element level focus on the evaluation of the effective properties as well as the generic sandwich behavior with respect to the damage tolerance, i.e. damage resistance and growth behaviour.

3.1. Determination of Effective Properties

For the purpose of sensitivity studies, a meso-mechanical analysis is carried out with parameterised FE models. The pins are described as a beam (1D) or as a solid element (3D) in the FE model of unit cells, which is in other respects fully modelled in 3D elements.

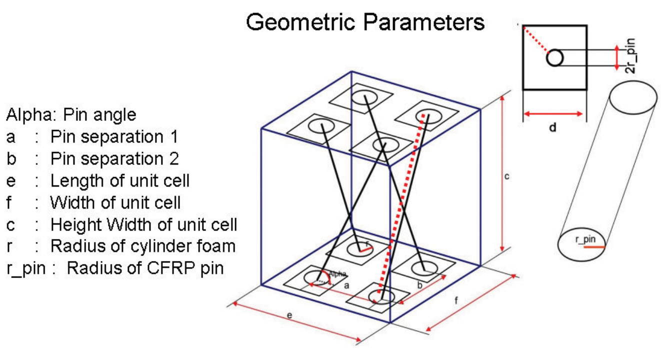

FIG. 15. Selectable parameters for the unit cells [20]

The selectable parameters (FIG. 15) are:

1) Pin angle α
2) Foam thickness or height of the unit cell c
3) Pin separation (pitch)

3D modelled cylinders that are used later to link the pin elements and the 3D foam elements together surround the 1D pin elements. These are divided into two half-cylinders by a mid surface on which the line representing the pin lies (FIG. 16 top). In the 3D model, the following additional parameters come into play:

4) Radius r (in 1D-3D is defined in material card)
5) Edge length d of the prism
6) Thickness of the face skin

The full 3D model is less flexible due to the fact that the face skins are automatically subdivided depending on the pin angle. Changes in the cell geometry lead to differing severity of distortion of the face skin elements.

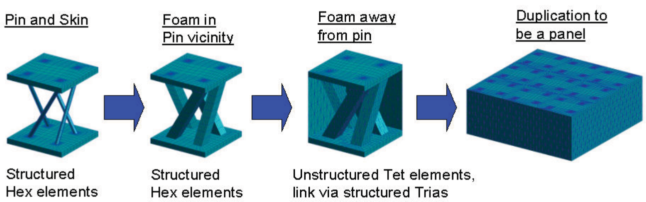

FIG. 16. Modelling of the pin with full 3D approach [20]

The convergence properties of the two modelling strategies are then investigated and contrasted. FIG. 17 shows that 1D-3D converges more quickly to one value. It lies however a long way below the realistic value or test re-

[14] Modified Vacuum Infusion

sults. The full 3D model converges only at element counts of 1 million or more, but shows a more realistic value [20].

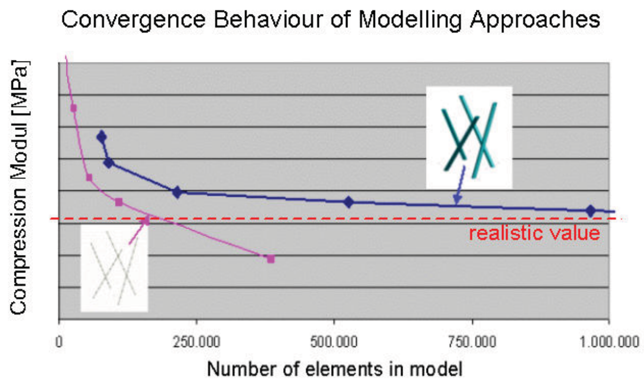

FIG. 17. Convergence of the two modelling approaches

Tests are carried out as per the specification in ASTM C365 for compression tests and ASTM C273 for shear tests. However, it was observed, that for reinforced sandwich the skin has stiffening effect on the test results. Embedding the top skin into a recess provided on the specimen support might be one way of minimising it.

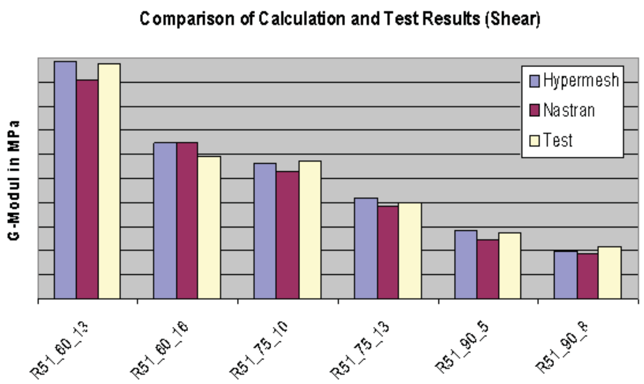

FIG. 18. Comparison of the test with the calculated results

A better correlation is demonstrated in shear stiffness than in the compression case as shown in FIG. 18 [19]. Besides the influence of skin stiffness, the anisotropy due to pin configurations may affect the effective compression properties. The full 3D model is therefore used to investigate the accompanying global torsion of the specimen under compressive or thermal loading, which may influence the effective stiffness up to 3% as shown in FIG. 19.

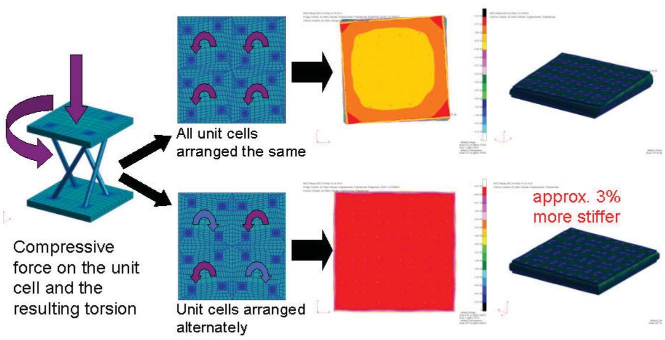

FIG. 19. Influence of the pin reinforcement configuration (anisotropy) on the calculated properties [20]

3.2. Investigation of the Impact Behaviour

FIG. 20. Impact testing of sandwich CAI-specimens

Sandwich specimens have demonstrated sufficient residual strength in compression after impact (CAI) testing [21]. Despite this there is still a strong motivation to simulate the impact behaviour of small specimens, FIG. 20, in order to develop design guidelines for impact resistance sandwich structures. For this purpose a discrete modelling approach was used to describe core reinforcements. The reasoning behind this is that in order to describe the impact behaviour correctly, the interaction of reinforcements and the foam core has to be taken into account. In consequence pins have been modelled as beam elements while embedded longitudinal profiles have been described using shell elements.

3.2.1. The Construction of The FE Model

Applying the aforementioned strategy of using discrete reinforcements a numerical model of the sandwich has been created using the explicit FE code LS-DYNA, FIG. 21, The design of the model was done similarly as described in [23] for an unreinforced model. Focus of the performed investigations was core damage, as it appears to be most critical for damage tolerance behaviour of the overall structure.

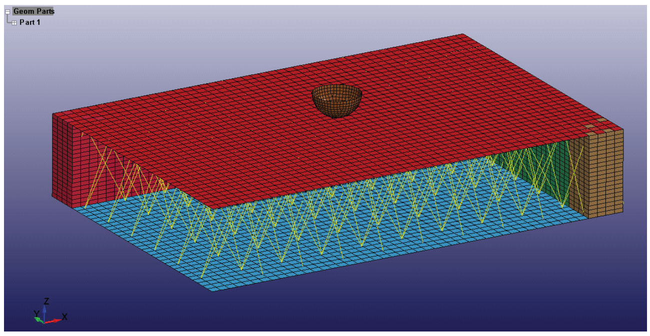

FIG. 21. FE-Model of a sandwich structures with pin reinforcements for impact investigations

Two issues that gained high importance during built-up of the model were the description of the pin-face skin interface as well as the interaction of the pins with the foam core. As a first approach displacements of the pins, modelled as beam elements, were directly coupled to the foam core using shared nodes. This however led to unrealistic results as the significantly more stiff pins destroyed the foam locally [24]. This was mostly due to the selected material model for the foam core, which however may not be altered significantly in order to keep a good global description of the foam damage. Therefore the direct coupling of pin and core displacements was cancelled and each pin was described by a single beam element in order to reach sufficient bending stability. This allows describing the core stiffness correctly in that pins and foam are applied in a parallel connection similar to that of two springs between plates.

The second issue was the connection of the pins to the face skins. In a similar manner the first approach was to couple the displacements of the pins and the face skins directly to each other. From experimental results it was however known that a few pin connections fail at or nearby the indentation of the impactor. In consequence simply coupling pins and face skins makes their connection too strong. Thus a cohesive zone model is applied to couple pin and face skin displacements until a maximum load per pin is reached. Above this load the connection is released describing a pin-face skin interface failure.

3.2.2. Comparison to Experiments

The discussed numerical model simulates experiments as described in [21]. The introduced pins are also made of CFRP and are applied at an inclination angle of 30° to the normal, which describes a good compromise between reinforcing shear and compression properties of the foam core. The pins have an approximate diameter of 2 mm leading to a reinforced foam density of 110 kg/m³.

In order to check the maturity of the selected modelling approach force vs. time data of the experimental impact and the numerical simulation have been compared (FIG. 22). In the beginning of the simulation a clearly detectable deflection in both simulated curves indicates early core damage due to local core indentation. Even though such a clear indication is missing within the experimental data, a slight curvature of the load curve also indicates irreversible processes [24].

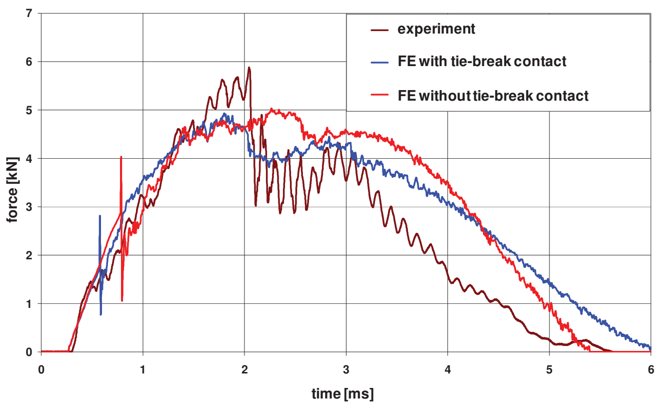

FIG. 22. Load vs. time data of a 16J impact on a pin reinforced sandwich structure

A sudden drop in the load curve following the global maxima at about 2 ms can be observed in the experimental data. This can be explained by face skin cracking occurring at this point. Additional failure of some pin-face skin interfaces within the numerical model supports this reasoning. A first estimation for the maximum load per pin interface was determined from [25]. Application of this modelling technique to larger sandwich structures is feasible and may be performed.

3.3. Investigation of Face Skin / Core System Disbonding (Crack Growth Behaviour)

The disbonding behaviours of interface skin to core system are investigated in order to evaluate the various reinforcement elements in Chapter 2.1. The investigations are based upon the Single Cantilever Beam (SCB) test for mode-I (peeling) and the Cracked Sandwich Beam (CSB) test for mode-II (shear) loading. The SCB and CSB tests are a special case or adaption of the well-known Double Cantilever Beam (DCB) and End Notched Flexure (ENF) tests respectively. The initial crack was realised by a teflon foil placed between top face skin and core [26, 27].

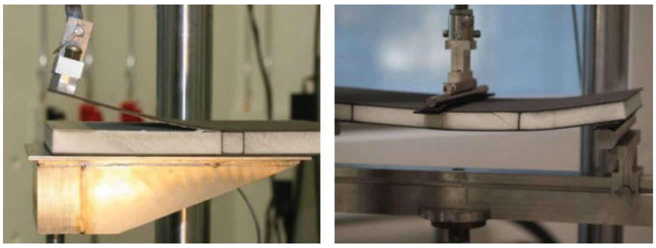

FIG. 23. Test setup of reinforced sandwich specimen [28]

3.3.1. Determination of Crack Length

The crack length was determined using the compliance method. The energy release rate ***G*** is the derivative of the compliance with respect to the crack length [26]

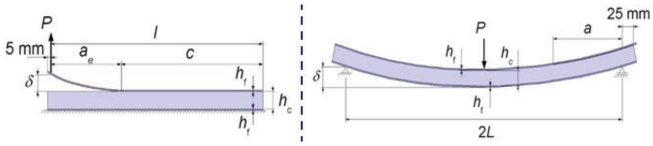

FIG. 24. Deformation in the DCB (a) and SCB test (b) [26]

Note: the quasi-static ultimate load (**P**) for the specimens' test is far beyond the design ultimate load (DUL) level.

3.3.2. Stiffness-Crack Length Curves

The use of the compliance method for the CFRP/foam core sandwich structure was then proved experimentally and numerically. The FE analysis was also used to calculate the energy release rate via Virtual Crack Closure Technique (VCCT), shown in following FIG. 25.

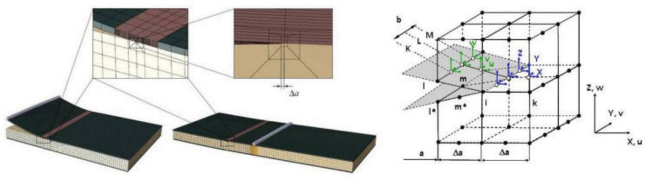

ERR VCCT-Mode-I-Component:

FIG. 25. FE analysis and the FE model of VCCT [29]

The comparison of the analytical, numerical and experimental compliance curves in 0 affirms the used of the compliance method, which will be transferred further in order to investigate large-scale sandwich component and with the reinforcement or crack stopper concepts.

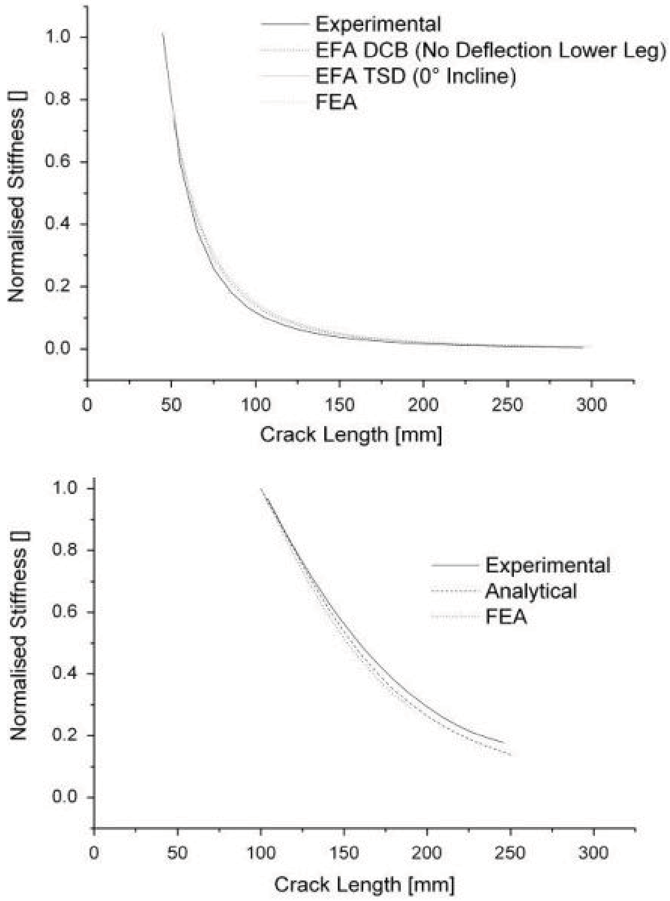

FIG. 26. Various results of compliance-crack length curves of the SCB (top) and CSB (bottom) [26]

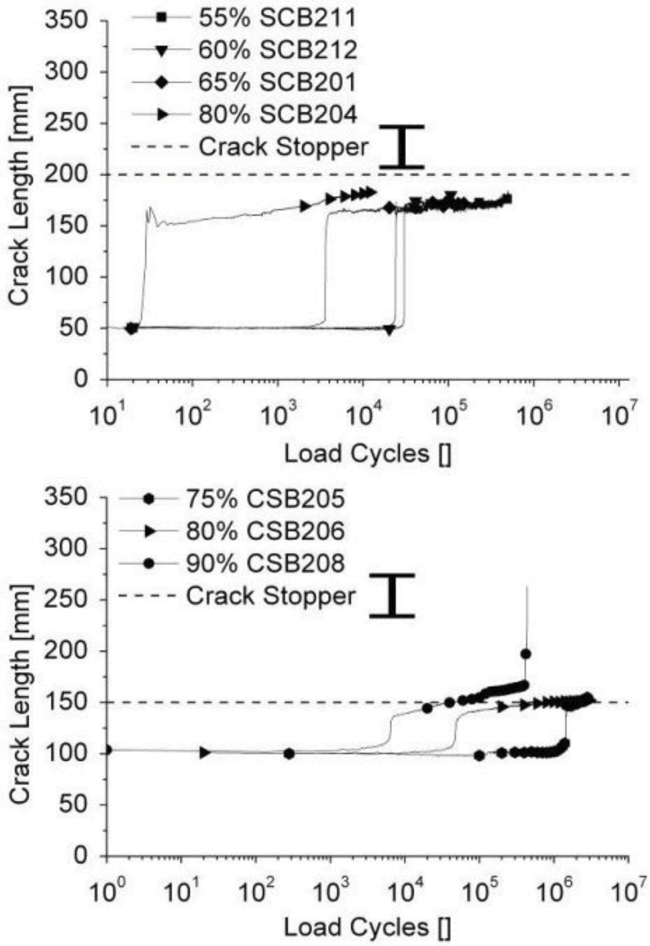

FIG. 27. Crack length-load cycle curves of double-T beam in SCB (top) and CSB (bottom) test as semi logarithmic plot [29, 30]

3.3.3. Fracture Toughness

The SCB (Eq. 8) and the CSB (Eq. 10) fracture toughness amount to 430 J/m² and 300 J/m² respectively. The mode II fracture toughness is much lower than mode I. Additionally, the influence of the face skin thickness on the crack propagation behaviour was investigated with SCB specimens having face skins up to 3.0 mm thick. However, no significant skin thickness effect was determined. All specimens failed in the same way.

3.3.4. Characterisation of Crack Stop Elements

The quasi-static tests indicated the best crack stop functionality of the double-T beam [26, 28]. The analysis results of unreinforced sandwich specimens are then used as basis for investigating the double-T reinforced ones with the same load ratio (***R***) of 0.1. The fatigue crack growth behaviour is quasi-brittle. The crack propagation was arrested in acceptable number of load cycles at 65 % of the load level shown in FIG. 27 (top). At the 75 and 80 % load level the crack stopper didn't fail after 3 million load cycles shown in FIG. 27 (bottom), which reveals the excellent crack stop capability of double-T reinforcement.

The results highlight the novel crack stop capability for the foam core of composite sandwich in anticipating any potential damage scenario within the design service goal of the advanced VTP and even its extended service goal.

4. INVESTIGATION OF DETAIL- AND SUB COMPONENT PARTS (MACRO-MECHANIC)

The investigations on detail and sub component level focus on the evaluation of the buckling stability as well as the strength with respect to the damage tolerance capability. By implementing the material properties and composite foam sandwich characteristics investigated in the previous chapter linear and also non-linear FE analysis are conducted. The results contribute to the development of calculation method for the advanced VTP centre box [31].

4.1. Shear-Compression Panel (Detail)

To verify the buckling stability, the sandwich panels are subjected incrementally to load cases acc. to TAB 2 [31].

Load Case	Compression [%]	Shear [%]
1	0	100
2	30	95
3	60	85
4	85	50
5	95	20
6	100	0

TAB 2. Load cases (combination of comp. and shear)

These shear-compression load combinations allow the construction of an interaction curve as shown in FIG. 2, in order to explore the possible reserve factors of composite sandwich structures with a unique lenticular cross section.

4.1.1. The Construction of the FE Model

The FE model of the sandwich panel is constructed through a solid shell strategy (2D-3D model); the foam core is modelled with solid elements and the CFRP skins with shell elements (FIG. 28), where the nodes of both element types merged in the interface. There is thus an incompatibility regarding rotational degrees of freedom. This is, however, still acceptable in case of hard foam cores, and any inaccuracy is yet minimised if the foam core is reinforced. For reinforced sandwich configurations, the effective material properties determined in Chapter 3.1 are applied. The loads are introduced into the sandwich panel with the help of constraint or RBE3[15]-elements.

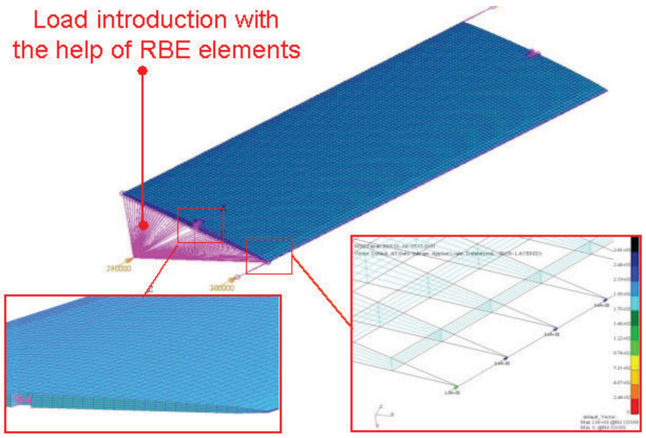

FIG. 28. Solid-Shell modelling and MPC element

4.1.2. Linear FE Buckling Analysis

The linear buckling modes calculated using the NASTRAN SOL 101 for the first three load cases or load combinations are found at the panel edge and are distinguished by shear buckling modes. As anticipated, the pure shear load causes a buckling mode inclined at 45° as shown in FIG. 29 (LH) and its buckling value is the largest of all load cases, which can be seen as non-critical. The last three load cases, on the other hand, initiate buckling modes that are distinguished by compressive buckling modes arising in the centre of the panel (FIG. 29 RH). The pure compressive load correspondingly causes a buckling mode inclined at 0° and its buckling value is the smallest, which is the critical one [32].

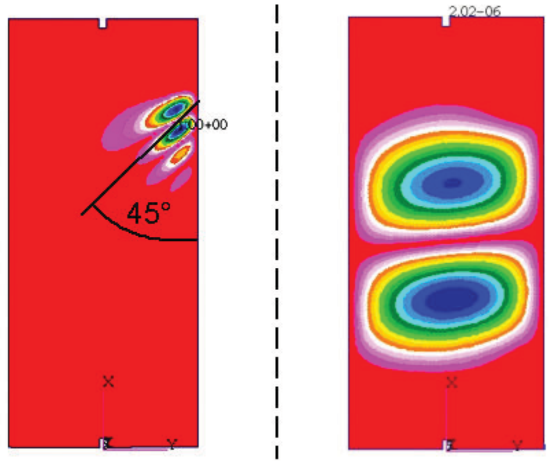

FIG. 29. Buckling modes under pure shear load or LC-1 from TAB 2 (LH) and LC-4 from TAB 2 (RH) [32]

4.1.3. Non-linear FE Buckling Analysis

Using the same FE model construction, a non-linear buckling calculation is carried out with the help of the ABAQUS FE code in order to generate the load-shortening curve, which will be later compared with the test results. The evaluation of calculation results shows that the mentioned FE model is equally suitable for the linear buckling analysis (*eigenvalue*, FIG. 29) and for the non-linear buckling analysis (*load increment*, FIG. 31).

4.1.4. FE Analysis with Impact Damage Models

The impact damage investigated in the section 3.2 is to be modelled in the shear-compression sandwich panel. Due to high computational effort and the corresponding transfer procedure has been not yet verified; only the damage size is transferred for the sake of convenience. With the help of the scripting language of the FE program, impact damage patterns investigated in section 3.2 including conical shear crack are semi-automatically embedded as sub-model into the FE model of sandwich panel. The material properties are reduced to less than 1% of the original undamaged material. A convergence analysis was conducted to verify the numerical stability of the damage model due to the stiffness discontinuities that arises as a result, as shown in FIG. 30.

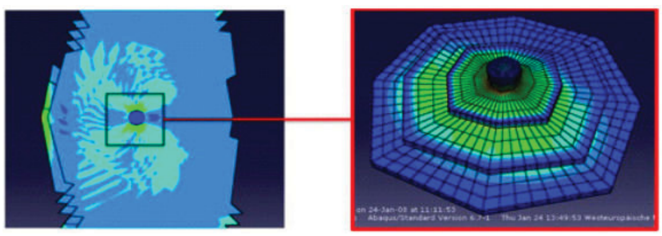

FIG. 30. Sub-model of damage pattern (shear crack) [19]

The FE stability analysis using the damage sub-model shows almost no change in structural response to the critical compressive loading. It is possible to see from the buckling modes that the position of the damage has virtually no effect on the global buckling stability of the sandwich panel. Even where there are two applied impact damage points or more, there is no weakening effect or deterioration of the composite sandwich structure.

[15] Rigid Body Element and interpolation elements respectively

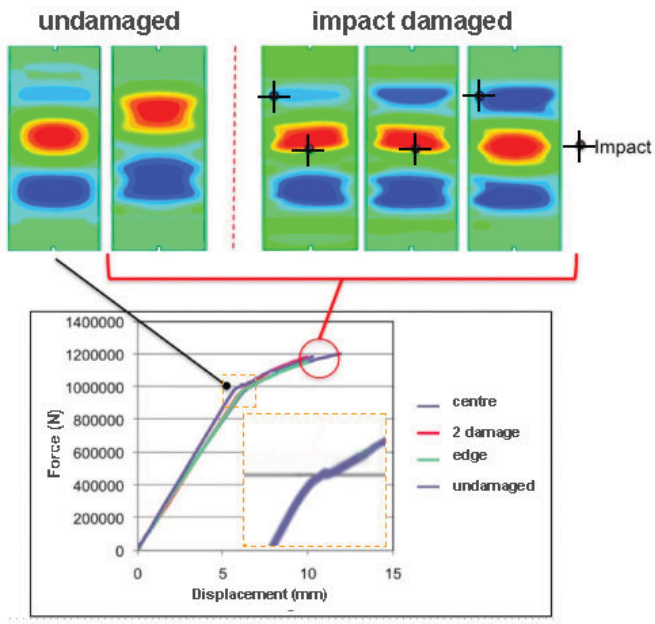

FIG. 31. Force-displacement diagram and buckling modes for a compressive load [19]

Through the intensive investigations of experimental and numerical results, it will be possible, that the impact damage simulation procedure on small specimens, as explained in chapter 3.2, is properly transferred into the FE model of a large-scale composite sandwich structure. This means that the scaling and curvature effects on the impact behaviour could be taken into account [32, 33, 34, 35 and 36]. A procedure for transferring the calculation of impact damage and its growth behaviour from small to actual large-scale sandwich component is to be developed in order to assess its damage tolerance properly.

4.1.5. Shear-Compression Test Results

To verify the selected modelling approach, the experimental results from the shear-compression tests are compared with the numerical results, as shown in FIG. 32.

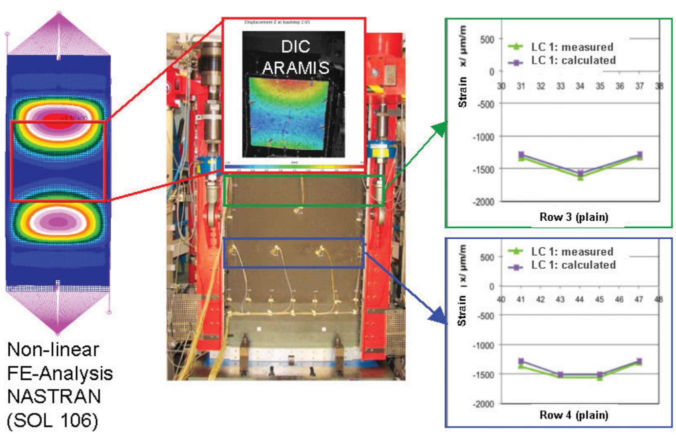

FIG. 32. Comparison between the FE calculation and measurement of strains and deformations

As predicted by non-linear stability analysis, the strain measurements show absolutely no change in structural response. Even with six impact-loading points[16], four of them with energy of 35 Joules, the load-strain diagrams are almost identical. It is noticeable, that the damage sizes are much less than the damages in the tests with small flat sandwich specimens [36] and only one side of the skin was damaged, which leads to comparatively advantageous load redistribution in the impacted zone.

The load-shortening curves (FIG. 33) show a fully linear behaviour of both the flat and curved skin up to load factor (**j**) of 2.2. The flat skin is slightly more deformed than the curved one. Even after fatigue test with 8000 simulated flight cycles or 48000 load cycles and ***R*** = 0.1 the structural response remains unchanged, which confirms the investigation results of good damage growth behaviour described in section 3.3. Only at very high load level (**j** = 2.5), shortly before the structure fails, the buckling onset occur with the corresponding out of plane displacement about 5mm, which was also recorded by a digital imaging camera system of ARAMIS®, FIG. 32.

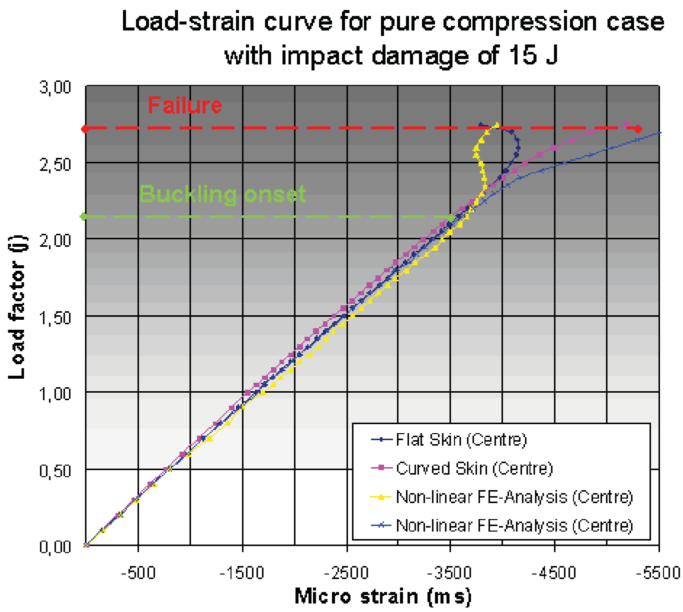

FIG. 33. Load-shortening curve at the centre of the panel. The rupture load is within the load factor (j) = 2.7

There was no post buckling identified prior to failure. The fracture initiation took place in the transition area of two half-waves with different phase, FIG. 34.

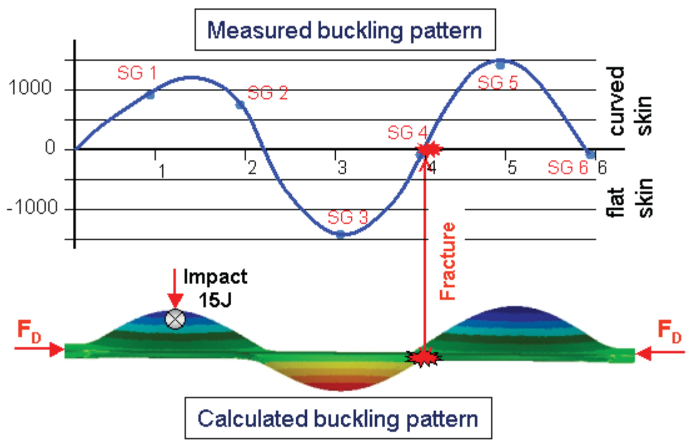

FIG. 34. Comparison between the measured buckling pattern and the computed one at rupture load.

[16] Multiple impact damages capability

The rupture load lies at a load factor (j) of 2.70 (FIG. 33). After the division of Ultimate Load Factor (UL) of 1.5, the resulted reserve factor (RF) is (2.7/1.5) = **1.8**. This result most closely matches the reserve factor determined in Chapter 2.2.2.6 and also confirms the applicability of the proposed structural calculation method. Tests with other load combinations of TAB 2 are conducted in order to construct the interaction curve of the sandwich structure.

Note: since the FE buckling analysis takes the influence of transverse shear into account, the resulting interaction curve will look like the dotted line shown in the FIG. 2.

4.2. Load Introduction Panel (Sub Component)

The strength and stability behaviour of load introduction or sandwich to monolithic transition area was also investigated using FE analysis and then compared to the test results. In order to avoid the application of large amount of solid elements in modelling the complex sandwich lay-up of the test panel, it is modelled using layered shell elements. Like the GFEM, the FE meshing of load introduction test panel results in a stepwise topography. The load transfer elements are realized via MPCs (RBE).

The structural response under combined axial and transversal loads is fully acceptable regarding strain allowable.

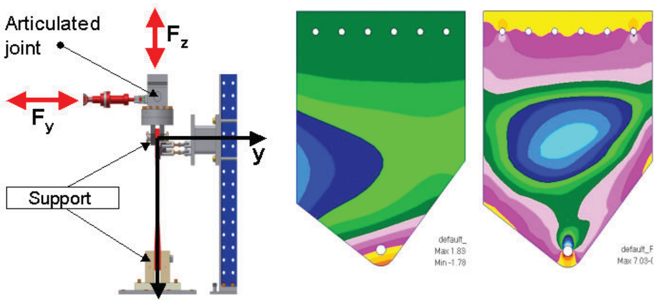

FIG. 35. The displacement in Y direction (LH) and the strain in Z direction of model with -Z_{ZX} offset [38]

After covering the opened edge of test panel with thin laminate to reduce the edge effect [39], test results show a linear structural deformation with maximum deviation to the FE model with a –t/2 offset method (FIG. 36).

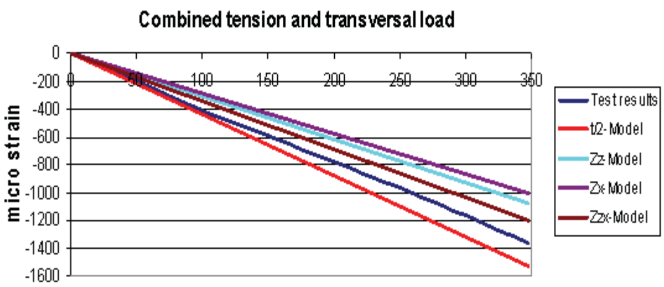

FIG. 36. Linear strains behaviour of the test result and the comparison to different offset methods [38]

5. SUMMARY AND OUTLOOK

State of the art numerical analysis method incorporating *multi-scale* modeling technique as well as *global-local* approach w.r.t test pyramid is successfully applied in the structural development of an advanced composite foam core sandwich structure. *Meso-mechanical* FE analysis, particularly the full 3D model, can be applied to determine the effective material properties of the pin-reinforced foam cores as well as their configuration-related thermo mechanical effects. Furthermore, the modeling strategy can be extended with an appropriate modification for investigating impact resistance and damage growth behaviour (durability).

The stability analysis of sandwich panels with reinforced foam cores is carried out, as far as computing time is concerned, with the homogenized FE model, i.e. *macro-mechanic*. Using the 2D-3D modelling approach, a good agreement between the analysis and test results can be achieved for the sandwich panel with a unique lenticular cross-section. The configuration is then simplified to apply the analytical calculation methods from standard structural handbook (HSB) for a purpose of sensitivity study.

Observed results show numerically and experimentally negligible effect of present impact damages on the global sandwich panel behaviour and its failure mechanism. Impact damage up to 35J has no discernible influence on the stability behaviour of the panel, not even when several impact points are applied (*Multiple Impacts Capability*). Also the deformation responses remain almost linear in all the cases investigated, event after fatigue or cyclic loading of 8000 flight cycles. The investigation results of the baseline configuration highlight the potential of the developed composite foam sandwich design principle of an advanced VTP centre box to be introduced into next generation commercial aircrafts [40].

6. KEY TO SYMBOLS

$\underline{u}_i$	Displacement vector at the node
$\delta \underline{u}_i$	Virtual displacement vector at the node
$\underline{u}^e$	Sum of the displacements at the nodes
$\underline{\sigma}$	Stress vector
$\underline{\underline{D}}$	Operator matrix
$\underline{\underline{E}}$	Matrix of material properties
$\underline{X}$	Volume force vector
$\underline{\underline{N}}_i$	Form function of a node
$\underline{\underline{N}}$	Matrix of the sum of all form functions
V	Volume of the component
O_P	Surface area of the component
$\underline{\underline{K}}^e$	Stiffness matrix of the total system
$\underline{\underline{K}}_L$	Linearly independent portion of the rigidity matrix
$\underline{\underline{K}}(\underline{u})^e$	Portion of $\underline{\underline{K}}^e$ which dependent on $\underline{u}^e$

7. ACKNOWLEDGEMENTS

The work presented in this paper was partially funded by **CTC GmbH** Stade and the **BMWi**, *Bundesministerium für Wirtschaft und Technologie* (Federal Ministry for Industry and Technology of Germany) with the support code **20W0605**. The authors wish to acknowledge this support.

REFERENCES

[1] M. I. Zuardy, P. C. Zahlen, C. Mudra, A. S. Herrmann: Strukturmechanische Analyse eines hochintegrierten Sandwichpaneels für die Luftfahrtanwendungen, German Aerospace Congress (DLRK), Hamburg, 2010

[2] J. Klammer, H. Baier: Vibroakustik und Wärmetransport Doppelschaliger CFK-Rümpfe, Lehrstuhl für Leichtbau, TU München, 2003

[3] W. Wohlers: Mehrstufige Optimierung komplexer strukturmechanischer Probleme, Dissertation, RWTH Aachen, 2005

[4] E. F. Bruhn: Analysis and Design of Flight Vehicle Structures, Purdue University, Jacob Publishing, Indianapolis, 1973

[5] W. L. Ko: Mechanical and Thermal Buckling Analysis of Sandwich Panels Under Different Edge Conditions, NASA Technical Memorandum 4535, California, 1993

[6] H. Razi, S. Ward: Principles for Achieving Damage Tolerant Primary Composite Aircraft Structures, The Boeing Company, Seattle, Washington, 2000

[7] T. S. Lim, C. S. Lee , D. G. Lee: Failure Modes of Foam Core Sandwich Beams under Static and Impact Loads, Journal of Composite, Vol. 38, No. 18, 2004

[8] D. Zenkert: An Introduction to Sandwich Construction, Chameleon Press LTD, London 1995

[9] T. Stöven, H. Wilmes, U. Hellwege, N. Kunze, G. Patzelt, J. R. Balzer, A. Herrmann, P. Zahlen, B. Kolesnikov, A. Fink, L. Herbeck, M. Kleineberg, G. Ernst: Kastenträger eines aerodynamischen Flächentragwerks, DE102005015337A1, Deutsches Patent- und Markenamt (DPMA), 2006

[10] J. A. Kepler: Sandwich / Catenary Hybrid Beams – Stiffness assessment and experimental verification, ICSS 9, Pasadena, California, USA, 2010

[11] L. E. Stanley, D. O. Adams: Development and Evaluation of Stitched Sandwich Panels, NASA, CR-2001-211025, Langley Research Center, 2001

[12] B. Castanié, J. J. Barrau, J. P. Jaouen, S. Rivallant: Combined Shear/Compression Structural Testing of Asymmetric Sandwich Structures, Society for Experimental Mechanics, Vol. 44 Nr. 5, Springer 2004

[13] J. Rouchon: "Certification of Large Airplane Composite Structures, Recent Progress and New Trends in Compliance Philosophy", ICAS 17, Stockholm 1990

[14] P. Middendorf: Entwicklung von FVK-Strukturen im Flugzeugbau, Presentation of EADS-IW at Structures Engin., Production & Mechatronics of TU-Wien, 2008

[15] C. Ledermann: Parametric Associative CAE-Methods in Preliminary Aircraft Design, Dissertation, ETH Zürich, 2006

[16] N. N: Handbuch Struktur Berechnung (HSB), Beulen ebener Rechteckplatten unter einachsigem Druck, 45111-02 A , IASB, 1985

[17] W. Oesmann, A. Koetzke: Druck-Schubanlage zur Einleitung von hohen Schublasten in ein vorzugsweise gewölbtes Flugzeugbauteil, EP1524513A2, European Patent Office, 2005

[18] B. J. Habibie: Einführung in die Finite Elementen Methode, Hamburger Flugzeugbau, Hamburg, 1968

[19] A. Paul: Nichtlineare Strukturanalyse von einfach gekrümmten CFK-Sandwichstrukturen, Diplomarbeit, TU-Braunschweig, 2008

[20] P. Abel: Mesomechanische Modellbildung pin-verstärkter CFK-Schaumsandwichs mittels FEM, Studienarbeit, RWTH Aachen, 2010

[21] J. Leijten, et al.: Experimental study of the low-velocity impact behaviour of primary sandwich structures, TU Delft, Composites: Part A, Elsevier, 2009

[22] T. B. Block, M. I. Zuardy, A. S. Herrmann: Impactuntersuchung von CFK-Sandwichstrukturen mit verstärkten Schaumkernen, DLRK, Hamburg, 2010

[23] T. B. Block, M. Calomfirescu, M. I. Zuardy, A. S. Herrmann: Simulation des Impactverhaltens von CFK-Sandwichstrukturen, DLRK, Aachen, 2009

[24] T. B. Block, C. B. Nguyen, M. I. Zuardy, P. C. Zahlen, A. S. Herrmann: FE-Analysis of the impact behavior of sandwich structures with pin-reinforced foam cores, ECCM IV, Paris, 2010

[25] A. I. Marasco: Analysis and evaluation of mechanical performance of reinforced sandwich structures: X-Cor and K-Cor, PhD Thesis, Cranfield University, 2005

[26] M. Rinker, M. John, R. Schäuble: Untersuchungen zur Schadenstoleranz von CFK-Schaumsandwichstrukturen mit Hilfe von DCB- Und ENF-Tests, German Aerospace Congress (DLRK), Hamburg, 2010

[27] L. A. Carlsson, L. S. Sendlein and S. L. Merry: Characterization of Face Sheet/Core Shear Fracture of Sandwich Beam, Journal of Composite Materials, 25, 101-116, 1991

[28] M. Rinker, M. John, P. C., Zahlen and R. Schäuble: Face sheet disbonding in CFRP/PMI sandwich structures under quasi-static and fatigue loading considering residual stress, Paper submitted for publication.

[29] M. Rinker, P. C., Zahlen, M. John and R. Schäuble: Investigation of Sandwich Crack Stop Elements under Fatigue Loading, Paper submitted for publication.

[30] M. Rinker, M. John and R. Schäuble, "Investigation of Sandwich Crack Stop Elements under Fatigue Loading", ICSS 9, Pasadena, California, USA, 2010

[31] M. I. Zuardy, P. C. Zahlen, A. S. Herrmann: Stabilitätscharakteristik eines fortschrittlichen Sandwichpaneels für die Luftfahrtanwendung, German Aerospace Congress (DLRK), Aachen, 2009

[32] D. Heber: Stability Characteristics of Plain-Curved Sandwich Panel, Diplomarbeit, FH-Aachen, 2007

[33] J. S. Tomblin, K. S. Raju, J. Liew, B. L. Smith: Damage Resistance & Tolerance of Composite Sandwich Panels – Scaling Effects, DOT/FAA/AR-03/75, 2004

[34] N. N.: Structural Size Effects, Chapter 7 – Damage Resistance, Durability and Damage Tolerance, MIL-HDBK-17-3F, Volume 3 of 5, DoD, USA, 2002

[35] R. C. Moody, J. S. Harris, A. J. Vizzini: Scaling and Curvature Effects on the Damage Tolerance of Impacted Composite Sandwich Panels, Journal of Sandwich Structures And Materials, Vol. 4 – 2002

[36] M. I. Zuardy, P. C. Zahlen, A. S. Herrmann: Skalierungs- und Krümmungseffekt zur Schadenstoleranz der Sandwichbauweise (ein Überblick), German Aerospace Congress (DLRK), Aachen 2009

[37] T. Bäumler: Fiber Metal Laminate Structures – from Laboratory to Application, Royal Aerospace Society Hamburg Branch, 2009

[38] M. Wald: Strukturanalyse einer komplex geformten CFK-Sandwich Lasteinleitung innerhalb eines Seitenleitwerkes nächster Generation, Diplomarbeit, FH-Aachen, 2009

[39] K. Rohwer, On the determination of edge stresses in layered composites, Technical Report, DFVLR, Braunschweig, 1981

[40] M. I. Zuardy, P. C. Zahlen, W. Vöge, A. S. Herrmann: Eine hochentwickelte CFK-Sandwichbauweise für hauptlasttragende Luftfahrtstrukturen, German Aerospace Congress (DLRK), Hamburg, 2010